

NDB

NAGW-1953

7N-91-CR

024 653

## *Impact-induced melting of planetary surfaces*

John D. O'Keefe and Thomas J. Ahrens

*Lindhurst Laboratory of Experimental Geophysics, Seismological Laboratory 252-21, California Institute of Technology,  
Pasadena, California 91125*

### ABSTRACT

The objective of this paper is to determine the thickness of the melt layer relative to the crater diameter for simple and complex craters. A numerical code was employed to calculate the amount of melting and the crater geometry. We used the code results and the scaling formalism of Holsapple and Schmidt (1987) to determine the scaling laws for the relative melt layer thickness.

Simple crater dimensions are dominated by impact parameters and the planet's strength, whereas complex crater dimensions are dominated by planetary gravity, strength, and the impact parameters.

The volume of melt is proportional to impact energy for impact velocities and melt enthalpies of interest to planetary science. Crater geometry and dimensions scale with an exponent,  $\mu$ , which is intermediate between momentum ( $\mu = 1/3$ ) and energy ( $\mu = 2/3$ ) scaling. For simple craters, the melt layer thickness/crater diameter,  $T/D$ , for a given planetary surface (constant melt enthalpy and mean impact velocity), is independent of the crater size. For complex craters,  $T/D$ , for a given planetary surface (constant melt enthalpy, impact velocity, and gravitational acceleration), increases with the size of the crater. For simple craters, at a fixed size, the relative melt layer thickness,  $T/D$ , increases slowly with increasing impact velocity,  $U$ , according to  $\propto U^{0.1}$ , whereas, for complex craters ( $\propto U^{0.22}$ ).

### INTRODUCTION

Previous investigators have examined impact-induced melting of planetary surfaces with a focus on the total amount of melt produced and the depth into the planet of melting. The focus of this study is to relate the crater observables both from remote observations and earth crater measurements that are associated with melting, with the nonobservables that can be calculated from detailed computer models.

Data related to impact melting on other planets that are observable remotely are limited. The spatial extent of the melt pool within the crater can be inferred by the change in the surface reflectance properties. Because the depth of melting cannot be measured remotely, the melt volume that remains within the crater can not be calculated. In the case of flooding of the melt outside the crater rim, crude estimates of the external melt volume can be made from assumptions of the local topography. In any case, the total melt volume and the depth

of melting are not observable and have to be inferred from modeling of the impact process. The other major crater observables are the crater diameter, and ring positions for complex craters and the equilibrated (after rebound) depth.

In the case of Earth impacts, the ability to make field measurements helps quantify some of the aspects of melting. The melt layer thickness within the crater at various locations can be determined from drill hole measurements. From these measurements, estimates of the volume of melt within the crater can be made. The volume of melt that is ejected outside the crater cannot be easily measured. Part of the melt is ejected in the high-speed ejecta sheet which becomes unstable and breaks up into fine particles, via hydrodynamic instabilities induced by the ejection process. These instabilities form as a result of molten ejecta interaction with the impact-induced vapor plume (for high-velocity impacts) or the planet's atmosphere (O'Keefe and Ahrens, 1982). These melt particles can be widely dispersed as in the case of tektites. Even estimating the amount of

O'Keefe, J. D., and Ahrens, T. J., 1994, Impact-induced melting of planetary surfaces, in Dressler, B. O., Grieve, R.A.F., and Sharpton, V. L., eds., *Large Meteorite Impacts and Planetary Evolution*: Boulder, Colorado, Geological Society of America Special Paper 293.

melt in the close-in ejecta blanket is difficult to quantify because of mixing with unmelted rock fragments. The depth of impact-induced melting within the planetary surface prior to modification by the cratering process is sometimes an observable. It is an observable when there is a well-defined layering sequence that can be used to reference the position of the melt boundary. The other major observables for terrestrial craters are the diameter, crater profile, distribution of shock-induced seismic wave velocity deficits resulting from rock cracking, and various degrees of shock metamorphism detectable as a function of position as observed via various microscopies.

The specific objective of this paper is to determine the thickness of the melt layer relative to the crater diameter. The diameter is almost always an observable and, as pointed out previously, the melt layer thickness is an observable for some terrestrial impacts.

The scope of this paper is to calculate the ratio of melt layer thickness to crater diameter,  $T/D$ , for simple and complex craters. Simple crater dimensions are dominated by the planet's strength and the impactor size and velocity, whereas for complex craters, final dimensions are dominated by the planet's gravity and strength, and the impactor size and velocity. For simple craters we calculated the melt layer thickness at the time of maximum penetration which also occurs at the end of the crater development. For complex craters we also calculated the melt layer thickness at the time of maximum penetration; however, in this case, the crater will rebound, and the observed melt layer thickness will be slightly greater. We carried out the calculations to the point where the crater diameter had stopped growing, but the crater floor was still moving upward and had not come to rest.

We examined the normal impact of spherical projectiles

onto a similar composition semi-infinite planetary surface material. The model did not include the planet's atmosphere; this would not strongly affect the melt layer in the crater, but would be important in the dispersal of the melt ejecta. We used an Eulerian-Lagrangian code (CSQ) developed by Thompson (1979) to calculate the pressure, density, particle velocity, and thermal energy fields as a function of time. The equation of state parameters are given in Table 1. In all cases the planet and impactors were similar materials and were at normal density (e.g., not porous).

We carried out this series of calculations over a broad range of impact conditions. These calculations are discussed in detail in O'Keefe and Ahrens (1993) and are listed in Table 1. The key parameters are the impactor velocity ( $U$ ), impactor radius ( $a$ ), planetary strength ( $Y$ ), gravity ( $g$ ), and the enthalpy required for ambient conditions to completely melt ( $H_m$ ). We used the scaling framework of Holsapple and Schmidt (1987) to develop scaling laws in the various impact regimes. The impact parameters and the dimensionless parameters are also defined and listed in Table 1. The magnitude of the three dimensionless parameters  $ga/U^2$ ,  $Y/\rho U^2$ ,  $H_m/U^2$  are measures of the dominant mechanisms controlling the cratering process. The inverse Cauchy number,  $Y/\rho U^2$ , is a measure of planetary strength relative to the impact pressure forces; the inverse Froude number,  $ga/U^2$ , is a measure of the gravitational forces relative to the impact pressure forces; and the melt number,  $H_m/U^2$ , is a measure of the magnitude and relative importance of melting. In determining the range of calculations, we had a choice of either varying the projectile size or the gravitational acceleration; for ease of computation we varied the gravitational acceleration over six orders of magnitude, which is equivalent to varying the impactor radius from 5 m to 5,000 km. In determining the range of

TABLE 1. SCOPE OF PARAMETERS STUDIED FOR IMPACT OF SILICATE PROJECTILE ON A PLANETARY HALFSPACE

Parameter	Symbol	Values Employed	Units
Impact velocity	$U$	12	km/sec
Planetary gravity	$g$	0, 1, $10^2$ , $10^4$ , $10^5$ , $10^6$ , $\times g_e$	$g_e$ (980 cm/sec <sup>2</sup> )
Density	$\rho$	2.7	g/cm <sup>3</sup>
Bulk modulus	$E$	$7.6 \times 10^{11}$	dynes/cm <sup>2</sup>
Gruneisen coefficient	$\gamma$	2.0	.....
Melt enthalpy	$H_m$	$1.1 \times 10^{10}$ $1.1 \times 10^{11}$	ergs/g
Yield strength	$Y$	0, 0.24, 2.4, 5.6, 24, 28, 140, 240, 2,400	kbar
Inverse Froude Number	$\frac{ga}{U^2}$	0.0, $3.4 \times 10^{-7}$ , $3.4 \times 10^{-5}$ , $3.4 \times 10^{-3}$ , $3.4 \times 10^{-2}$ , $3.4 \times 10^{-1}$	.....
Inverse Cauchy Number	$\frac{Y}{\rho U^2}$	0.0, $6.2 \times 10^{-5}$ , $6.2 \times 10^{-4}$ , $1.4 \times 10^{-3}$ , $6.2 \times 10^{-3}$ , $7.2 \times 10^{-3}$ , $3.6 \times 10^{-2}$ , $6.2 \times 10^{-2}$ , $6.2 \times 10^{-1}$	.....
Melt number	$\frac{H_m}{U^2}$	$7.4 \times 10^{-3}$ , $7.4 \times 10^{-2}$	

the melt number, we restricted the impact velocity to 12 km/sec so as to not get into the impact regime where significant amount of vaporization would occur. For silicates, this restricts the range over which the scaling laws are accurate to velocities less than 30 km/sec.

## BACKGROUND

O'Keefe and Ahrens (1977) examined the impact melting of planetary surfaces and found that the total volume ( $V_m$ ) of melt scaled as the energy of the impactor ( $U^2$ ). Subsequently, Bjorkman (1984) and Bjorkman and Holsapple (1987) examined this problem from the framework of their coupling theory. They predicted that the relative melt volume should scale as follows:

$$\frac{V_m}{a^3} \propto \left[ \frac{H_m}{U^2} \right]^{-3\mu_m/2} \quad (1)$$

where  $\mu_m$  is an exponent to be determined from either experiment or calculations. When  $\mu_m = 0.66$ , the volume of melt is proportional to the energy of the impactor; when  $\mu_m = 0.56$  to 0.58, the volume of melt scales in between energy and momentum scaling, and it scales in the same manner as the other aspects of the cratering process do at late times. These other aspects include the depth, diameter, and crater lip height (e.g., O'Keefe and Ahrens, 1993; Holsapple, 1993).

To understand why the melt volume did not scale in the same manner as the other aspects of the cratering process at late times, Bjorkman and Holsapple (1987) carried out a series of calculations in which they varied the velocity from 5 to 100 km/sec. They concluded that the total volume of the melt scaled with the energy of the impact up to velocities approaching 50 km/sec. The latter velocity is near the upper limit of interest in planetary impact cratering. At velocities greater than 50 km/sec, the melt volume was found to approach the same scaling relation as other aspects of the crater evolution at late times. They attributed this lack of consistency with the coupling theory at lower velocities due to the failure of the point source approximation. The point source approximation is used in the coupling theory of Holsapple and Schmidt (1987). The point source approximation is not expected to provide a good description of phenomena that occur close to the impactor and have spatial scales on the order of or less than the impactor size. Physically, the reason for this difference is that most of the melting occurs during the penetration of the projectile for conditions typical of planetary impacts. During penetration, the interface between the impactor and the planet grows linearly with time. This occurs for dimensionless times,  $\tau = Ut/a \lesssim 5$ . During penetration and for  $\tau \lesssim 5$ , cratering phenomena scale with impactor kinetic energy. However, for  $\tau \gtrsim 5$ , release waves from the free surface of the planet and the back of the projectile will overtake the expanding shock wave and cause the wave to decay more rapidly. It is well known that the con-

ditions behind the shock wave are subsonic, and release waves will always overtake the shock. The minimum decay of the shock wave would occur for energy scaling and the maximum for momentum scaling. The coupling theory gives shock-wave decay rates that are in between these two limits.

In summary, the volume of melt, which is produced at early times, scales as the energy of the impactor for most situations; however, the observable, which is the configuration of the crater produced at late times, scales as less than energy scaling, and from our previous series of calculations (O'Keefe and Ahrens, 1993), is well described by the Holsapple and Schmidt point-source formalism.

## SCALING RELATIONS

From Equation 1, the thickness of the melt layer ( $T$ ) scales as

$$\frac{T}{a} = K_m \left[ \frac{H_m}{U^2} \right]^{-\mu_m/2} \quad (2)$$

Under conditions where  $H_m/U^2 > 4 \times 10^{-4}$  (Bjorkman and Holsapple, 1987), then the melt layer exponent  $\mu_m$  is equal to 0.66, which results in energy scaling. This is the situation for most planetary impacts, where  $H_m > 10^{10}$  ergs/g and  $U < 20$  km/sec, which gives  $H_m/U^2 = 2.5 \times 10^{-3}$ . When  $H_m/U^2 < 4 \times 10^{-4}$ , then the melt layer thickness exponent ( $\mu_m$ ) approaches the value of the coupling exponent ( $\mu$ ). This latter situation occurs for high-speed impacts and/or for hot planets.

## SIMPLE CRATERS

For simple bowl-shaped craters, the shape is dominated by the strength of the planet. The shape of a simple crater at the end of its growth, along with contour plot of the associated enthalpy field is shown in Figure 1. The diameter ( $D$ ) of the crater scales as

$$\frac{D}{a} \propto \left[ \frac{Y}{\rho U^2} \right]^{-\mu/2} \quad (3)$$

where  $\mu$  is the coupling exponent of Holsapple and Schmidt (1987). The melt layer thickness relative to the crater diameter is obtained by dividing Equation 2 by Equation 3 giving

$$\frac{T}{D} = K \left[ \frac{Y}{\rho U^2} \right]^{\mu/2} \left[ \frac{H_m}{U^2} \right]^{-\mu_m/2} \quad (4)$$

An example of the melt layer thickness at the end of crater growth is shown in Figure 1. Using these results to evaluate  $K$  and rearranging Equation 4 gives

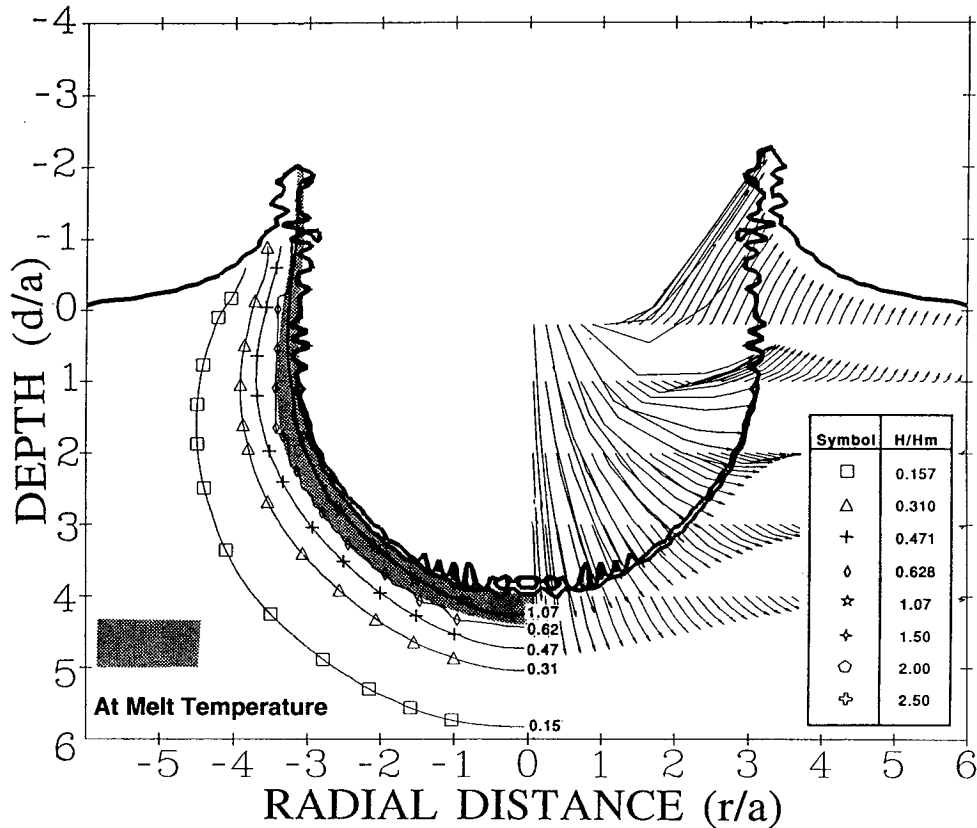


Figure 1. Simple crater near the end of crater growth,  $\tau = 16$ . Here  $\tau$ , normalized time, is  $\tau = tU/a$ , where actual time since impact is  $t$ . The inverse Cauchy number is  $1.44 \times 10^{-3}$  and the inverse Froude number is  $3.7 \times 10^{-7}$ . Shown in the figure are enthalpy fields and tracer particle trajectories. Left: Contours of enthalpy, normalized to enthalpy required to melt from ambient temperature. Shaded region is at temperatures greater than the melt temperature. Right: Displacement of material from the initial position. Arrows indicate direction of displacement.

$$\frac{T}{D} = 7.8 \times 10^{-2} \left[ \frac{Y}{\rho H_m} \right]^{\mu/2} \left[ \frac{H_m}{U^2} \right]^{-(\mu_m - \mu)/2} \quad (5)$$

For most situations of interest in planetary impact ( $H_m/U^2 > 4 \times 10^{-4}$ ), the melt exponent,  $\mu_m$  is 0.66 (energy scaling) and the coupling exponent,  $\mu$  is 0.56 (O'Keefe and Ahrens, 1993; Holsapple, 1993). This gives  $\mu/2 = 0.28$  and  $(\mu_m - \mu)/2 = 0.05$ . For simple craters,  $T/D$ , for a given planetary surface (constant melt enthalpy and impact velocity), is independent of the crater size. The value of  $T/D$ , for a constant melt enthalpy and impact velocity, increases with the planet's strength. That is, the amount of melting is constant (and is established at early times) and the melt thickness is then determined by the size of the crater cavity which is controlled by the strength. Note that for this case there is a weak velocity dependence,  $\propto U^{0.1}$ ; for an order of magnitude increase in velocity there is only a 25% increase in relative melt layer thickness. For very high speed impacts and/or hot planets, ( $H_m/U^2 < 4 \times 10^{-4}$ ), then  $\mu_m = \mu$ , and the relative thickness is independent of velocity. Equation 5 is plotted in Figure 2, for various values of  $H_m/U^2$ .

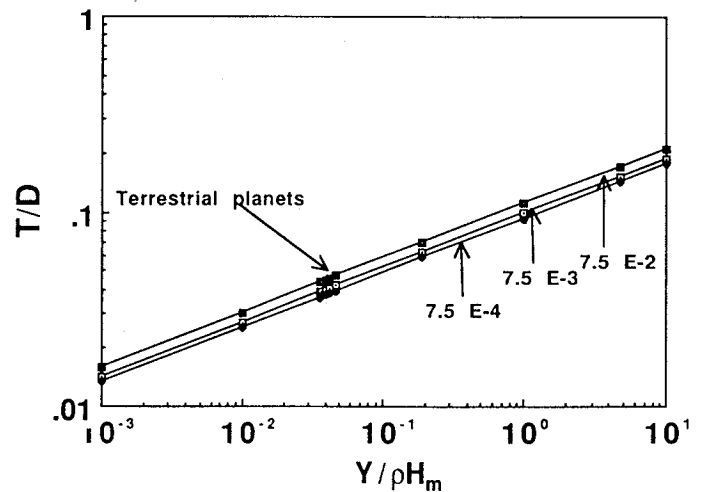


Figure 2. Simple crater melt layer thickness,  $T$ , divided by crater diameter,  $D$ , as a function of  $Y/\rho H_m$  for various values of  $H_m/U^2$ . The melt coefficient ( $\mu_m$ ) was taken to be 0.66 and the coupling coefficient ( $\mu$ ) was taken to be 0.56.

## COMPLEX CRATERS

For complex craters, gravity plays a dominant role in determining the transient crater diameter and depth of penetration and is balanced by strength forces in determining the final shape. The shape of a typical complex crater at the time of maximum penetration, along with contour plots of the enthalpy field is shown in Figure 3.

The final crater diameter for nominal planetary crustal strengths scales as

$$\frac{D}{a} \propto \left[ \frac{ga}{U^2} \right]^{-\mu/(2+\mu)} \quad (6)$$

The melt layer thickness relative to the final crater diameter is given by dividing Equation 2 by Equation 6, yielding

$$\frac{T}{D} = K \left[ \frac{ga}{U^2} \right]^{\mu/(2+\mu)} \left[ \frac{H_m}{U^2} \right]^{-\mu_m/2} \quad (7)$$

The constant  $K$  as before was evaluated from the code runs; an example of the melt layer thickness at the time of maximum penetration is shown in Figure 3. From these results,  $K = 0.75$ .

Rearranging Equation 7 gives

$$\frac{T}{D} = 0.75 \left[ \frac{ga}{H_m} \right]^{\mu/(2+\mu)} \left[ \frac{H_m}{U^2} \right]^{-\mu^2/2(2+\mu)} \left[ \frac{H_m}{U^2} \right]^{-1/2(\mu_m-\mu)} \quad (8)$$

Equation 8 is plotted in Figure 4. For a given average planetary surface (constant melt enthalpy, average velocity, and gravitational acceleration), the relative thickness of the melt layer increases with the size of the crater. This occurs because the thickness of the melt increases linearly with the radius, whereas the diameter of the crater increases at less than a linear rate with increasing impactor radius; the gravitational forces play a greater relative role with increasing crater size. In addition, for a fixed impactor size, constant gravitational acceleration and melt enthalpy, the relative thickness of the melt increases with impact velocity because more melt volume

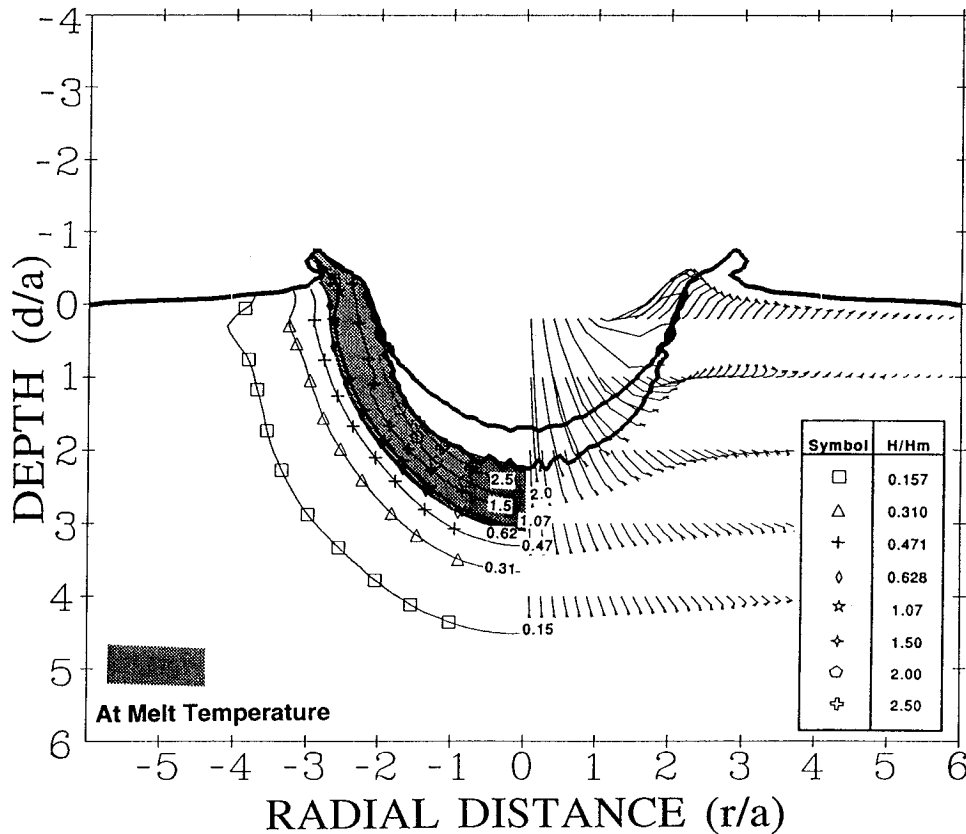


Figure 3. Complex crater at the time of maximum penetration in the gravity dominated regime,  $\tau = 10.2$ . Shown in the figure are the enthalpy field and tracer particle trajectories. The inverse Froude number is  $3.4 \times 10^{-2}$ , and the inverse Cauchy number is  $6.17 \times 10^{-3}$ . Other symbols are the same as in Figure 1. The shaded region is at temperatures greater than the melt temperature.

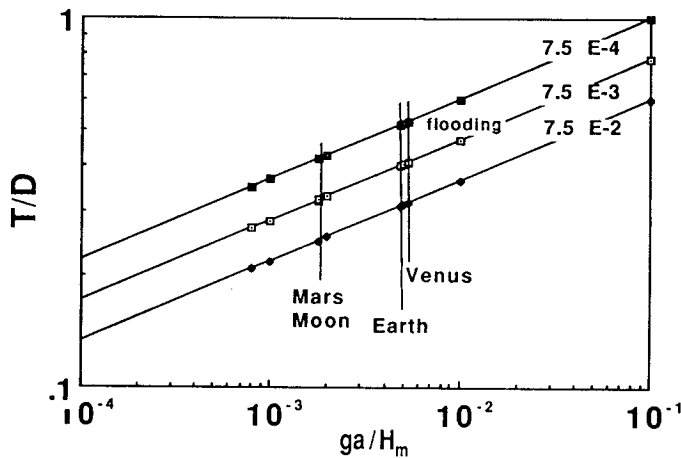


Figure 4. Complex crater melt layer thickness at the time of maximum penetration,  $T$ , divided by the final crater diameter,  $D$ , as a function of  $ga/H_m$  for various values of  $H_m/U^2$ . The melt exponent ( $\mu_m$ ) was assumed to be equal to 0.66 and the coupling exponent,  $\mu = 0.56$ . The lines on the figure are for the terrestrial bodies with the properties given in Table 2, and for an impactor radius of  $a = 1$  km.

is produced with increasing velocity than crater volume. For a fixed impactor velocity and impactor radius, the relative melt thickness increases with planetary gravity because the melt volume is independent of gravity, whereas, the crater volume decreases with gravitational acceleration. Thus, for a given impact condition, the relative melt layer thickness would be greater on planets with higher gravitational acceleration. The last term in Equation 8 accounts for the difference between en-

ergy and coupling parameter scaling. Note that as opposed to simple crater energy scaling, even if the last exponent is zero, the relative thickness is still a function of velocity.

### LATE STAGE MELT LAYER FLOODING

In gravity dominated craters, the gravitational forces cause a dynamic collapse of the transient crater cavity (O'Keefe and Ahrens, 1993) and if there is sufficient melting, flooding of the crater with melt occurs. Shown in Figure 5 is a gravity-dominated crater in the terminal phase of evolution. The melted region forms a pool of melt and because of the uplifting of the center of the crater can give rise to external flooding. The impact regime where melt flooding is expected is indicated in Figure 4.

### CONCLUSIONS

The volume of melt is proportional to the impact energy for velocities and melt enthalpies of interest to planetary science. The crater geometry scales with an exponent,  $\mu$ , which is intermediate between momentum ( $\mu = 1/3$ ) and energy ( $\mu = 2/3$ ) scaling. For simple craters, the melt layer thickness/crater diameter, for a given planet surface (constant melt enthalpy and mean impact velocity), is independent of the crater size. For complex craters, the melt layer thickness/crater diameter for given planetary surface (constant melt enthalpy, average velocity, and gravitational acceleration), increases with the size of the crater. For simple craters the relative melt layer thickness is weakly dependent upon velocity ( $\propto U^{0.1}$ ), and for complex craters, the relative melt layer thickness is also weakly dependent upon velocity ( $\propto U^{0.22}$ ).

TABLE 2. SHOCK-INDUCED MELT PARAMETERS FOR TERRESTRIAL PLANETS AND ICY SATELLITES

Object	Surface Gravity (cm/sec <sup>2</sup> )	Mean Asteroidal Impact Velocity (km/sec)	Dynamic Strength* (kbar)	Surface Temperature (°K)	Enthalpy to Melt 10 <sup>10</sup> (ergs/g)
Earth (An) <sup>†</sup>	980	18	35	250-310	2.04
Moon (An)	160	14	35	120-370	2.04
Mars (An)	370	10	35	200-245	2.10
Venus (An)	860	18	35	730	1.62
Mercury (An)	358	20	35	600	1.77
Europa (H <sub>2</sub> O)	130	19	2	124	0.57
Ganymede (H <sub>2</sub> O)	140	15	2	140	0.54
Callisto (H <sub>2</sub> O)	130	13	2	150	0.53

\*Hugoniot elastic limit value. This is the peak value. Fractured material will be weaker by a factor of 10<sup>-1</sup> to 10<sup>-2</sup>.

<sup>†</sup>An indicated anorthite silicate assumed. H<sub>2</sub>O indicates hexagonal ice.

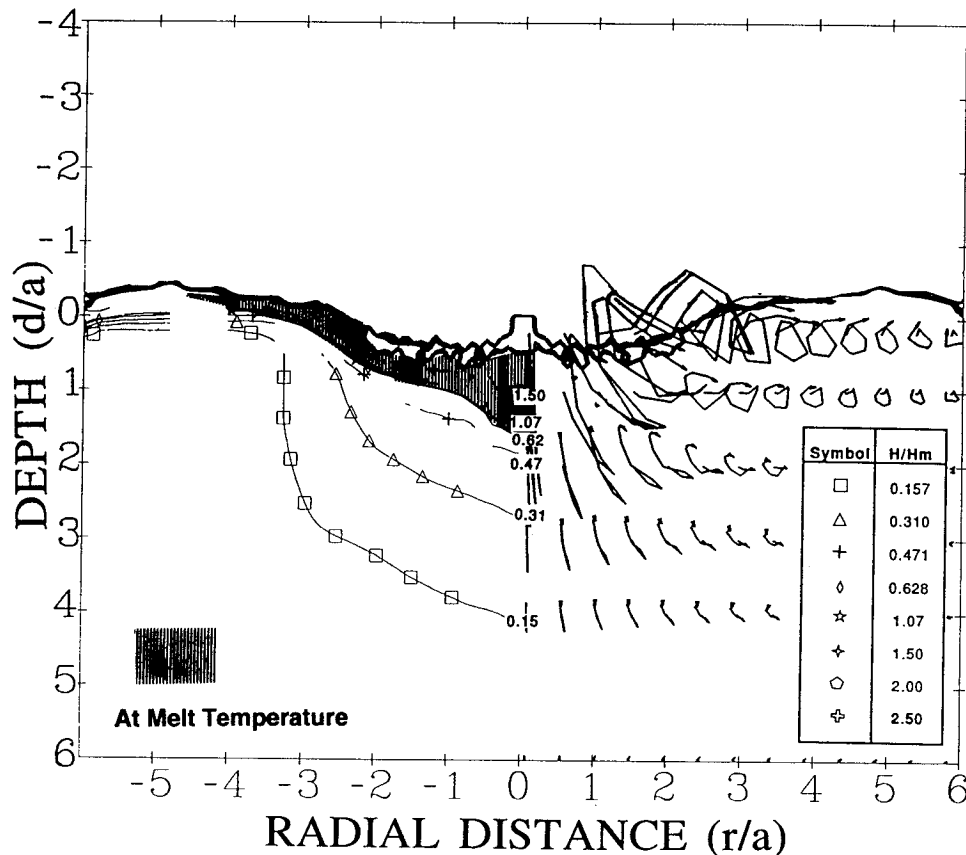


Figure 5. Impact-induced flow field in the terminal phase. Plot shows rebounding of gravity dominated crater and development of flooding of the melt layer onto surface at  $\tau = 50$ . The inverse Froude number is  $3.4 \times 10^{-2}$  and the inverse Cauchy number is  $6.2 \times 10^{-5}$ .

## ACKNOWLEDGMENTS

Research supported under NASA grant NAGW 1953. We appreciate the assistance of Michael Lainhart with the calculations. We thank W. W. Anderson for comments on the manuscript. This chapter is Contribution 5259, Division of Geological and Planetary Sciences, California Institute of Technology, Pasadena, California.

## REFERENCES CITED

- Bjork, R. L., Kreyenhagen, K. N., and Wagner, M. H., 1967, Analytic study of impact effects as applied to the meteoroid hazard: Washington, D.C., NASA, Contractor's Report, CR-757.
- Bjorkman, M. D., 1984, Feasibility of determining impact conditions from total crater melt [abs.]: Lunar and Planetary Science XV, p. 64-65.
- Bjorkman, M. D., and Holsapple, K. A., 1987, Velocity scaling impact melt: International Journal of Impact Engineering, v. 5, p. 155-163.
- Holsapple, K. A., 1993, The scaling of impact processes in planetary sciences, Annual Review of Earth and Planetary Sciences, v. 21, 333-374.
- Holsapple, K. A., and Schmidt, R. M., 1987, Point-source solutions and coupling parameters in cratering mechanics: Journal of Geophysical Research, v. 92, p. 6350-6376.
- O'Keefe, J. D., and Ahrens, T. J., 1977, Meteorite impact ejecta: Dependence on mass and energy lost on planetary escape velocity: Science, v. 198, p. 1249-1251.
- O'Keefe, J. D., and Ahrens, T. J., 1982, Interaction of the Cretaceous/Tertiary extinction bolide with the atmosphere, ocean and solid Earth: Boulder, Colorado, Geological Society of America Special Paper 190, p. 103-120.
- O'Keefe, J. D., and Ahrens, T. J., 1993, Planetary cratering mechanics: Journal of Geophysical Research, v. 98, p. 17,011-17,028.
- Orphal, D. L., Bordon, W. F., Larson, S. A., and Schultz, P. H., 1980, Impact melt generation and transport, in Merrill, R. B., ed., Physical processes, Proceedings, Lunar and Planetary Science Conference, Houston, Texas: Geochimica et Cosmochimica Acta Special Publication No. 11, v. 3, p. 2309-2323.
- Thompson, S. L., 1979, CSQII—An Eulerian finite-difference program for two-dimensional material response—Part 2. Energy flow sections: Albuquerque, New Mexico, Sandia National Laboratories, SAND 77-1340.

MANUSCRIPT ACCEPTED BY THE SOCIETY DECEMBER 28, 1993

